



# CONVOLUTION NEURAL NETWORK COMPARISON ANALYSIS FOR BONE FRACTURE DIAGNOSIS

Gujjula Swarnalatha<sup>1</sup>, Dr. S. Rangaswamy<sup>2</sup>

1. Ph.D scholar, Department of Computer Science, BEST Innovation University, Gorantla, Sri Sathyasai District, Andhrapradesh, swarnagujjula57@gmail.com
2. Associate Professor, Head of the Dept., Vignan's Institute of Management and Technology for Women, Hyderabad, Telangana.

## Abstract:

Identification of bone fractures with computer-aided detection and diagnosis is an utmost need of today. It helps radiologists in saving the time and improving the performance. There were many image processing techniques used earlier for detecting the bone fractures. In the current condition of medical imaging processing, models based on deep learning in specific convolutional neural networks are widely used. It also extends its horizon in bone fracture detection from the X-Ray images. The commonly used dataset for bone fracture detection is MURA Dataset. A computer-aided telemedicine system must include automated fracture identification. Human arbitrary bones frequently fracture as a result of unintentional trauma, such as sliding. In reality, many hospitals are short on qualified surgeons who can identify fractures. Computer-aided diagnosis (CAD) lessens the workload for medical professionals while also detecting fractures. In this study, several deep convolutional neural network models for fracture detection are evaluated. The MURA Dataset has been employed therefore in occurrence. Three models—two variations of the DenseNet169 model and a VGG Model—have been examined. The DenseNet model designed is differentiated from the standard model including the variation in the loss function and the usage of weights. This article specifically concentrates on the detection of fracture in humerus bone extracted from the MURA Dataset.

DOI Number: 10.48047/nq.2023.21.6.nq23195

NeuroQuantology2023;21(6): 1970-1976

## 1. INTRODUCTION

In order to ease the work of clinicians involved in detecting the fractures, computer assisted diagnostic and detection mechanisms are widely used. According to Joshi & Singh (2020) the different kinds of bone fractures are Explained. Major types of bone fracture It has been observed that, earlier conventional image processing methods are used for fracture detection, they are replaced by various machine learning models, now, Deep learning models are in practice for detecting the fractures[1].

## 2. DATA ACQUISITION

For this research, radiograph images of the elbow, finger, forearm, hand, humerus, shoulder, and wrists are taken using MURA Dataset. Pranav Rajpurkar *et al.* (2018) have employed DenseNet169 Model for predicting the abnormality. The objective of the work is to predict the fracture in the radiograph

images. The total numbers of studies are 14,863 which include all the images[2]. The radiograph image considered in the study Humerus. The reason for choosing the humerus bone fracture is that in order to develop a model that can effectively identify the fracture and classify at the best the fracture and non-fracture images by training with a small set of data.

This kind of model can be helpful in scenarios where there is non-availability of large dataset like MURA dataset with huge amount of studies that can be used for training the model[3]. The other factor that has been taken for consideration is most of the existing models and works are trained with the complete MURA Dataset which has X-Ray images of different types of bones.

Identifying of Radiograph images that contains hardware in it is an easy task for any one and it does not need any specialized radiologists. All the images that contains hardware similar to the one shown in Figure 1 (a) are removed



manually. But, the remaining cases have different types of fracture, the one that can be

identified are oblique type fracture[4].

Figure 1 Samples of humerus



(a) Abnormal(with fracture)



(b) Abnormal (with hardware)

Remaining can only be identified by the radiologists. The following Figure 2 represents the sample positive cases considered in the study. The Figure 2 (b) is easily identifiable by anyone and the one in Figure 2 (a) needs a radiologist to diagnose.



Figure 2 Sample of positive cases considered in the study.

After removing the images with hardware in it, the total number of patients remaining are 117 and the number of images is 240 images as few patients contains 3 studies. DenseNet169 Model is implemented in two variants, one that as actually specified in the Pranav Rajpurkaret *al.* (2020) and the other a little variant of it. Both are described below[5].

The total number of Radiograph images with



Figure 3 Horizontal flipping (a) Original image and (b) Flipped image

With the use of horizontal sampling, we have a total of 480 images in positive cases and 643 images in negative cases[6,7]. Studies have shown that in the works related to Mura dataset abnormalities are identified rather than specifically identifying the fracture. Hence, the training is done with all

no fracture is 643 which belong to 319 patients. The images are rescaled into 224 x 224. Since there is a class imbalance between the positive cases and the negative cases, Data Augmentation is applied in the positive cases by means of horizontal flipping as it is found to be effective as per (Bin Guan 2020). The following Figure 3 displays an instance of horizontal flipping generated in order to increase the number of images.

the images, but in this work the training of the models is done only with the positive case images that contain fractures and negative images that are without fractures. 1123 images make up the complete collection. 10% of the images are utilised as the test set, with remaining 90%

contributing towards model training.

**3. RELATED WORK**

The general architecture is given in the following Figure

4. The major layers that are used in the convolutional neural network are

- Convolution Layer
- ReLU Layer
- Pooling
- Flattening
- Full

Connection

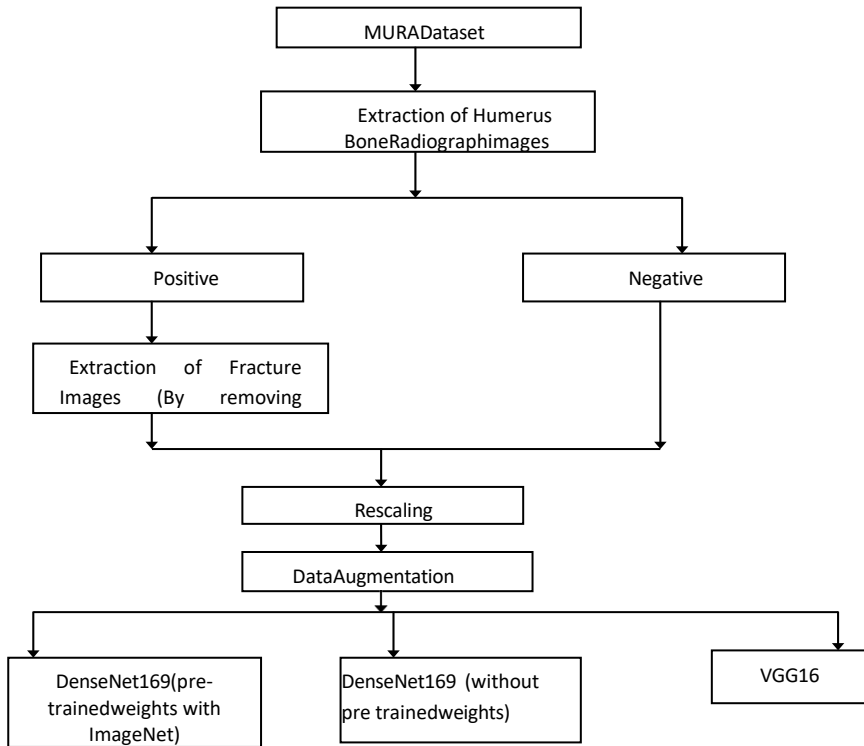


Figure4 Block diagram of proposed work

**4. METHODOLOGY**

The model employed are DenseNet169 as specific in the Muradataset. DenseNet is a kind of convolutional neural networks as given in Huang *et al.* (2017)[12]. The difference between the conventional neural

network and DenseNet is, in case of DenseNet there are 'l' number of inputs, for the layer 'l'. The inputs consists of the summarized feature maps that are collected from all the convolutional blocks that presides the l<sup>th</sup> layer of the DenseNet[13].

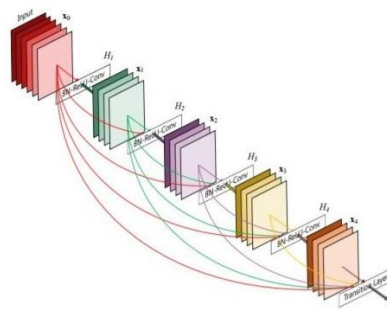


Figure 5. Dense block with 5 layers

It shows that each layer gets the feature map of the layers that comes before it. The main layers that has been used in the model are batch normalization, rectifier linear unit and convolution layers. The conventional neural network with the dense block can be represented as shown in the Figure 6, it is inferred from Gao Huang (2018)[14].



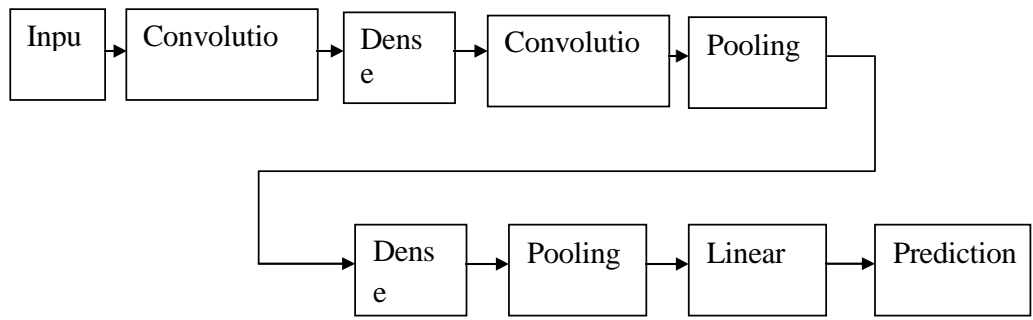


Figure6 Deep dense network

It can be observed from the figure that the densely connected models would have multiple dense blocks. The dense blocks are separated with the set of layers called as the transition layers. The transition layers may be the pooling layer or the convolution layer[15]. The layer may differ based on the application and need for the particular application.

The loss function that has been employed in the model is binary cross entropy rather than the actual weighted binary cross entropy that is used in the actual model Pranav *et al.* (2018). The binary cross entropy is represented in Equation (3)

$$\text{Lossfunction} = -\frac{1}{N} \sum_{i=1}^N y_i \cdot \log(p(y_i)) + (1 - y_i) \cdot \log(1 - p(y_i))$$

where,

- y is the label, 1 for the positive case and 0 for negative
- p(y) probability that the particular study belongs to a particular class.

The weights assigned are the pre-trained weights of DenseNet169 in ImageNet Dataset. 8 batch with a total of ten epochs are being used.. DenseNet169 model one with the pre-trained weights and the random weights are tested. Two variant of DenseNet169 are depicted in the Figure 7

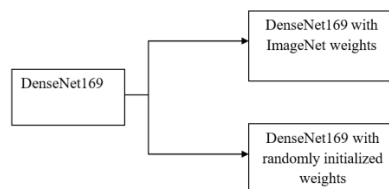


Figure7 DenseNet variations

Two models were tested one that uses the pre-trained Image Net and the one that uses weights assigned randomly the accuracy obtained with the same is given in the results section. As specified in the T. Urakawa, *et al.*(2018)[16], single output layer is used in the model instead of the prevailing fully connected layer. The results obtained with this model are discussed in the results section.

**4.1 VGG16 MODEL**

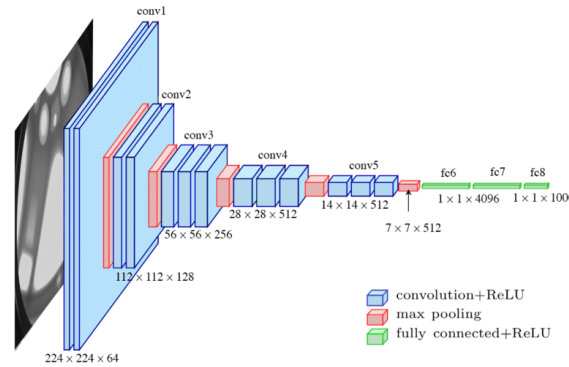
VGG16 model as designed in the B.M. Dhahir *et.al*(2014) [17] is another model used for detecting the fracture in the Humerus bone images. This model has proven to perform well in the ImageNet Dataset. There are series of convolution layers employed in the model, feed forward model is used for connecting all the layers. There are 2 blocks which



contains 2 convolutional layers and there are 3 blocks which contains 4 convolutional layers. The convolution layer depends on the stride 1 and 3 x 3 convolution. These

convolutional blocks are separated by the maxpooling layer.

Figure 8: VGG16 architecture



A softmax layer is at the end of the model to get an output and the operation defined in it is given in Equation (4).

where, 
$$J = -\frac{1}{m} \sum_{i=1}^m \sum_{j=1}^n y_j^{(i)} \log(y_j^{(i)}) + (1 - y_j^{(i)}) \log(1 - y_j^{(i)})$$

$y_j^{(i)}$  is the ith training label for output node j,

$y_j^{(i)}$  is the number of training / batch samples, n is the number of samples, and  $y_j^{(i)}$  is the ith predicted label for output node j.

4.2

DENSENET169

The models employed are DenseNet169 as specified in the Mura dataset. DenseNet is a kind of convolutional neural networks as given in Huang et al. (2017)[18]. The difference between the conventional neural network and DenseNet is, in case of DenseNet there are 'l' number of inputs, for the layer 'l'. The inputs consist of the summarized feature maps that are collected from all the convolutional blocks that precede the lth layer of the DenseNet.

The SoftMax layer is used for normalizing the

output value in the range from 0 to 1. The accuracy obtained with this model is provided in the next section. The same collection of images used in DenseNet are used for testing and training the model.

5. EXPERIMENTAL RESULTS AND DISCUSSIONS

The following Figures 12 and 13 give the accuracy obtained with the different models DenseNet169 with pre-trained weights of ImageNet, and DenseNet169 model without pre-trained weights.

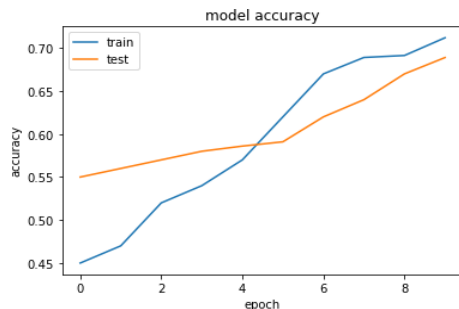


Figure 9 Model accuracy with random weights

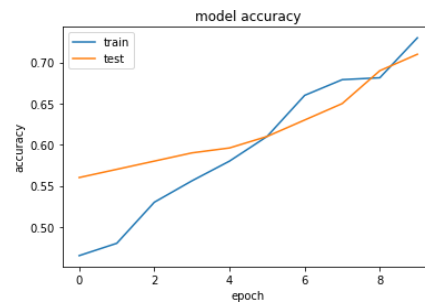
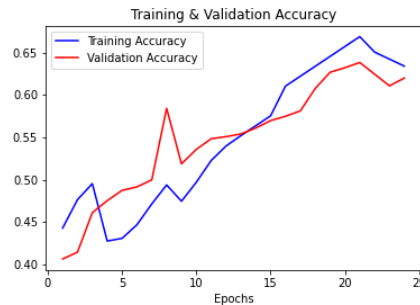


Figure 10 Model accuracy with pre-trained weights (ImageNet)



Figure 11 Model accuracy with VGG



The accuracy obtained with the VGG16 model is comparatively very less than the other models only 62% accuracy is obtained with it. The accuracy plot is shown in Figure 11.

The comparisons of the test accuracy of the three models are given in Figure 12

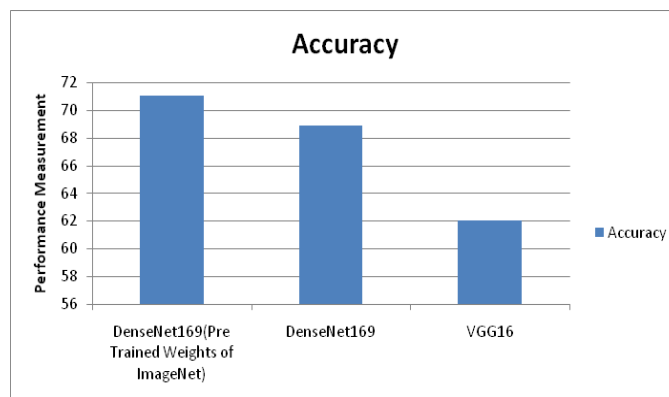


Figure 12 Accuracy of the models

But the accuracy obtained is not satisfactory. Improving the performance of the model will be the part of the future work. The Images considered for training is only the fracture images unlike the other studies which uses the entire MURA Dataset. The training images, though consider only the radiograph images of Humerus bone fractures it does not classify the fractures, it is believed that concentrating on a particular kind of fracture would increase the performance.

**6. CONCLUSION**

The utilization of various pre-trained models in the classification of humerus fractures is described in this article. The humerus bone fracture images are extracted from the MURA dataset and Pre-trained DenseNet and VGG16 model. The results are compared. The Analysis of eISSN1303-5150

the DenseNet model explained, is differentiated from the standard model including the variation in the loss function and the usage of weights.

**References:**

- [1]. Burr DB. Introduction - bone turnover and fracture risk. J Musculoskeletal NeuronallInteract 2003;3(4):408–9.
- [2]. Pranata YD, Wang K, Wang J, Idram I, Lai J, Liu J, Hsieh I. Deep learning and surffor automated classification and detection of calcaneus fractures in ct images. Comput Methods Progr Biomed 2019;171:27–37.
- [3]. E. Yahalomi, M. Chernofsky, M. Werman, Detection of distal radius fracturestrained by a small set of x-ray images and faster r-cnn., [arXiv: Computer Visionand Pattern www.neuroquantology.com



- Recognition].
- [4]. Urakawa T, Tanaka Y, Goto S, Matsuzawa H, Watanabe K, Endo N. Detecting intertrochanteric hip fractures with orthopedist-level accuracy using a deep convolutional neural network. *Skeletal Radiol* 2019;48(2):239–44.
- [5]. M. Margaliot, Bone fracture detection. Dahir BM, Hameed IH, Jaber AR. Prospective and retrospective study of fractures according to trauma mechanism and type of bone fracture. *Res J Pharm Technol* 2017;10(11):1994–2002.
- [6]. Bandyopadhyay O, Biswas A, Bhattacharya BB. Long-bone fracture detection in digital x-ray images based on digital-geometric techniques. *Comput Methods Progr Biomed* 2016;123:2–14.
- [7]. Wu J, Davuluri P, Ward KR, Cockrell C, Hobson R, Najarian K. Fracture detection in traumatic pelvic CT images. *J Biomed Imag* 2012;2012:1.
- [8]. Cao Y, Wang H, Moradi M, Prasanna P, Syeda-Mahmood TF. Fracture detection in x-ray images through stacked random forests feature fusion. In: *Biomedical Imaging (ISBI), 2015 IEEE 12th International Symposium on*. IEEE; 2015. p. 801–5.
- [9]. Umadevi N, Geethalakshmi S. Multiple classification system for fracture detection in human bone x-ray images. In: *Computing communication & networking technologies (ICCCNT), 2012 third international conference on*. IEEE; 2012. p. 1–8.
- [10]. Liang J, Pan B-C, Huang Y-H, Fan X-Y. Fracture identification of x-ray image. In: *Wavelet analysis and pattern recognition (ICWAPR), 2010 international conference on*. IEEE; 2010. p. 67–73.
- [11]. A. Oyeranmi, B. Ronke, R. Mohammed and A. Edwin, “Detection of Fracture Bones in X-ray Images Categorization,” *Journal of Advances in Mathematics and Computer Science*, 35(4): 111, 2020
- [12]. Huang Yi Yang and Ling Cheng, Long-Bone Fracture Detection Using Artificial Neural Networks Based On Line Features of X-Ray Images, 2019
- [13]. Gao, Wint Wah Myint, Khin Sandar Tun, Hla Myo Tun. Analysis on Leg Bone Fracture Detection and Classification Using X-ray Images. *Machine Learning Research*, Vol. 3, No. 3, 2018, pp. 49-59.
- [14]. Gao Huang, Y.D. Pranata, K. Wang, J. Wang, I. Idram, J. Lai, J. Liu, I. Hsieh. Deep learning and surf for automated classification and detection of calcaneus fractures in CT images. *Comput Methods Progr Biomed*, 171 (2019), pp. 27-37
- [15]. E. Yahalomi, M. Chernofsky, M. Werman, Detection of distal radius fractures trained by a small set of x-ray images and faster r-cnn., [arXiv: Computer Vision and Pattern Recognition].
- [16]. Y. Tanaka, S. Goto, H. Matsuzawa, K. Watanabe, N. Endo. Detecting intertrochanteric hip fractures with orthopedist-level accuracy using a deep convolutional neural network. *Skeletal Radiol*, 48 (2) (2019), pp. 239-244
- [17]. B.M. Dahir, I.H. Hameed, A.R. Jaber. Prospective and retrospective study of fractures according to trauma mechanism and type of bone fracture. *Res J Pharm Technol*, 10 (11) (2017), pp. 1994-2002
- [18]. Huang et al. Long-bone fracture detection in digital x-ray images based on digital-geometric techniques. *Comput Methods Progr Biomed*, 123 (2016), pp. 2-14

